

**Magnetic properties and magnetocaloric effects in GdCo<sub>9</sub>Si<sub>2</sub> compound with multiple magnetic phase transitions**

Z. G. Zheng, X. C. Zhong, J. L. Zhang, Z. W. Liu, V. Franco, and D. C. Zeng

Citation: [Journal of Applied Physics](#) **113**, 17A938 (2013); doi: 10.1063/1.4799973

View online: <http://dx.doi.org/10.1063/1.4799973>

View Table of Contents: <http://scitation.aip.org/content/aip/journal/jap/113/17?ver=pdfcov>

Published by the [AIP Publishing](#)

---

**Articles you may be interested in**

[Magnetic properties and magnetocaloric effect in the RCu<sub>2</sub>Si<sub>2</sub> and RCu<sub>2</sub>Ge<sub>2</sub> \(R=Ho, Er\) compounds](#)

J. Appl. Phys. **115**, 073905 (2014); 10.1063/1.4864419

[Magnetic properties and magnetocaloric effects in Er<sub>3-x</sub>GdxCo intermetallic compounds](#)

J. Appl. Phys. **113**, 033908 (2013); 10.1063/1.4776742

[Magnetic phase transitions and magnetocaloric properties of \(Gd<sub>12-x</sub>Tbx\)Co<sub>7</sub> alloys](#)

J. Appl. Phys. **109**, 07A919 (2011); 10.1063/1.3551736

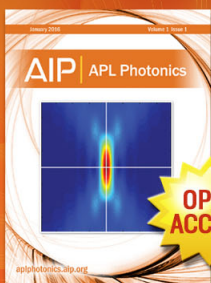
[Magnetic and magnetocaloric properties of Gd<sub>6</sub>X<sub>2</sub>Si<sub>3</sub> \(X=Ni, Co\) and Ln<sub>6</sub>Co<sub>2</sub>Si<sub>3</sub> \(Ln=Pr, La\)](#)

J. Appl. Phys. **109**, 07A913 (2011); 10.1063/1.3544509

[Thermopower behavior in the Gd<sub>5</sub>\(Si<sub>0.1</sub>Ge<sub>0.9</sub>\)<sub>4</sub> magnetocaloric compound from 4 to 300 K](#)

J. Appl. Phys. **91**, 4457 (2002); 10.1063/1.1459612

---



Launching in 2016!

The future of applied photonics research is here

OPEN ACCESS

**AIP** | APL Photonics

## Magnetic properties and magnetocaloric effects in GdCo<sub>9</sub>Si<sub>2</sub> compound with multiple magnetic phase transitions

Z. G. Zheng,<sup>1</sup> X. C. Zhong,<sup>1</sup> J. L. Zhang,<sup>2</sup> Z. W. Liu,<sup>1,a)</sup> V. Franco,<sup>3</sup> and D. C. Zeng<sup>1,a)</sup>

<sup>1</sup>*School of Materials Science & Engineering, South China University of Technology, Guangzhou 510640, People's Republic of China*

<sup>2</sup>*Department of Physics and Materials Science, City University of Hong Kong, Kowloon Tong, Hong Kong*

<sup>3</sup>*Department of Condensed Matter Physics, ICMSE-CSIC, Sevilla University, P. O. Box 1065, 41080 Sevilla, Spain*

(Presented 18 January 2013; received 5 November 2012; accepted 22 January 2013; published online 10 April 2013)

The structure and magnetic properties of polycrystalline GdCo<sub>9</sub>Si<sub>2</sub> compound have been investigated. It has a BaCd<sub>11</sub> structure and undergoes two magnetic phase transitions: an antiferromagnetic to ferrimagnetic transition occurring at ~93 K, and a ferrimagnetic to paramagnetic transition at 420 K, which results in a positive and a negative magnetic entropy change, respectively. The two peak values of magnetic entropy change are -0.6 and 1.1 J·kg<sup>-1</sup>·K<sup>-1</sup> for Δ*H* = 5 T. Furthermore, there exists a metal-semiconductor transition temperature (*T<sub>P</sub>*), below which the resistance increases with increasing temperature, while the semiconductor characteristic is observed above *T<sub>P</sub>*. The magnetic domain structures are characterized by stripe and grid structures 1 μm wide. Although the MCE is small for applications, its study is useful to clearly understand the nature of multiple magnetic phase transitions in the GdCo<sub>9</sub>Si<sub>2</sub> compound. © 2013 American Institute of Physics. [<http://dx.doi.org/10.1063/1.4799973>]

Magnetic materials with large magnetocaloric effect (MCE) have attracted considerable attention for potential applications in magnetic refrigeration. In recent years, excellent magnetocaloric properties have been observed in Gd and its compounds.<sup>1</sup> Due to their large magnetic moments and low anisotropy, Gd-based compounds are definitely prime candidates for achieving large MCE.<sup>2</sup> In a previous work, we have investigated the magnetic properties and magnetocaloric effect of compounds (Gd<sub>12-x</sub>Tb<sub>x</sub>)Co<sub>7</sub> (*x* = 0, 4, and 8),<sup>3</sup> amorphous Gd<sub>4</sub>Co<sub>3</sub> alloys,<sup>4</sup> and Gd<sub>65</sub>Mn<sub>35-x</sub>Ge<sub>x</sub> (*x* = 0, 5, and 10).<sup>5</sup> All families exhibited large magnetic entropy change (Δ*S<sub>M</sub>*). However, the high contents of transition metals generally lead to the decrease of saturations because of their ferrimagnetic nature. This point is clearly seen from the high saturated moment of Co-deficient compounds, such as Gd<sub>5</sub>CoSi<sub>2</sub>.<sup>6</sup> The compound shows a ferromagnetic ordering at 168 K and has large MCE with adiabatic temperature change Δ*T<sub>ad</sub>* = 5.9 K and magnetic entropy change -Δ*S<sub>M</sub>* = 8.7 J·kg<sup>-1</sup>·K<sup>-1</sup> for a magnetic field change of 4.6 T. Compared with Gd, transition metals show many practical advantages, such as lower material cost and larger corrosion resistance. There are previously published results for compounds in this system, such as Gd<sub>6</sub>Co<sub>2</sub>Si<sub>3</sub>,<sup>7</sup> GdCo<sub>13-x</sub>Si<sub>x</sub>,<sup>8</sup> and Gd<sub>6</sub>Co<sub>1.67</sub>Si<sub>3</sub>.<sup>9</sup> They have gained more attention as potential highly efficient magnetocaloric materials and giant isotropic magnetostriction materials.<sup>10</sup> This inspires us to investigate the magnetic behaviors of Co-rich compounds in the Gd-Co-Si system. However, except for above mentioned Gd-based compounds, only a few reports are available on the structure and magnetocaloric studies on this series. In this

work, we have synthesized the ternary silicide GdCo<sub>9</sub>Si<sub>2</sub>, and investigated its structure, magnetic properties and magnetocaloric effect in detail.

The compound GdCo<sub>9</sub>Si<sub>2</sub> was prepared by arc-melting a mixture of pure Gd (99.95 wt. %), Co (99.99 wt. %), and Si (99.99 wt. %) in argon atmosphere. To ensure compositional homogeneity, the ingots were repeatedly melted at least four times. Before characterization, the ingots were wrapped in Ta foil and annealed at 1000 °C for 5 days. The structure of the samples was identified by Philips X'pert Pro MPD X diffractometer. The microstructure was observed using scanning electron microscope (SEM) with energy dispersive spectroscopy (EDS) attached. The temperature and magnetic field dependences of magnetization were measured by a physical properties measurement system (PPMS-9, Quantum Design Co.). The electrical resistance measurement was done by the four probe method using PPMS. The magnetic force microscopy (MFM) and atomic force microscopy (AFM) measurements were performed with a commercial scanning probe microscope (Asylum Research, Cypher).

The X-ray powder diffraction pattern indicates that BaCd<sub>11</sub>-type GdCo<sub>9</sub>Si<sub>2</sub> (space group I41/amd) is the major phase, whilst there is still a minor phase of Co<sub>9</sub>Si (space group P63/mmc). The refined unit cell parameters for GdCo<sub>9</sub>Si<sub>2</sub> are: *a* = 7.932(2) Å and *c* = 6.287(8) Å, respectively. The estimated content of Co<sub>9</sub>Si is about 7 wt. %. The small amount of Co<sub>9</sub>Si, with a Curie temperature higher than 900 K, should make negligible contribution to the magnetic behavior of samples.

To confirm the contents of the impurity phase, the sample was also inspected using SEM/EDS. The back-scattered electrons image presented in Figure 1 confirms the composition of the major phase as 9.1 at. % of Gd, 73.8 at. % of Co,

<sup>a)</sup>Authors to whom correspondence should be addressed. Electronic addresses: zwliu@scut.edu.cn and medczeng@scut.edu.cn.

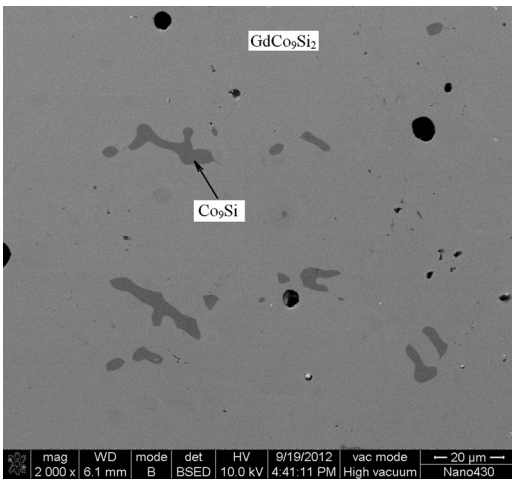


FIG. 1. Microstructure of the annealed sample. The major phase  $\text{GdCo}_9\text{Si}_2$  and the impurities  $\text{Co}_9\text{Si}$  are indicated. The black round areas correspond to the opened porosities.

and 17.1 at. % of Si, close to the exact formula of  $\text{GdCo}_9\text{Si}_2$ . The stoichiometry of the gray zone is found to be  $\text{Co}_9\text{Si}$ . The black round areas correspond to the open porosities, which may be formed in arc melting processes. The fraction of  $\text{Co}_9\text{Si}$  impurity was also estimated based on the SEM images to be less than 7%, in good agreement with results from X-ray diffraction.

Figure 2 shows the temperature dependence of zero field cooled (ZFC) and field cooled (FC) magnetizations for  $\text{GdCo}_9\text{Si}_2$  compound. The transition temperatures are derived from the extreme values of  $dM/dT$  vs  $T$  curves shown as the inset of Fig. 2. It is clear that the compound exhibited magnetic ordering below 420 K ( $T_{\text{SR}2}$ ), and a sharp drop of magnetic susceptibility was also evident at 93 K ( $T_{\text{SR}1}$ ). A small thermal irreversibility between ZFC and FC curves is observed below  $T_{\text{SR}2}$ , which may be attributed to the domain-wall pinning effect. It is indicated that the compound undergoes two magnetic phase transitions with increasing temperature: an antiferromagnetic to ferrimagnetic near  $T_{\text{SR}1}$  (Ref. 11) and then to paramagnetic transition at  $T_{\text{SR}2}$ . Above  $T_{\text{SR}2}$ , perfectly paramagnetic behavior was observed,

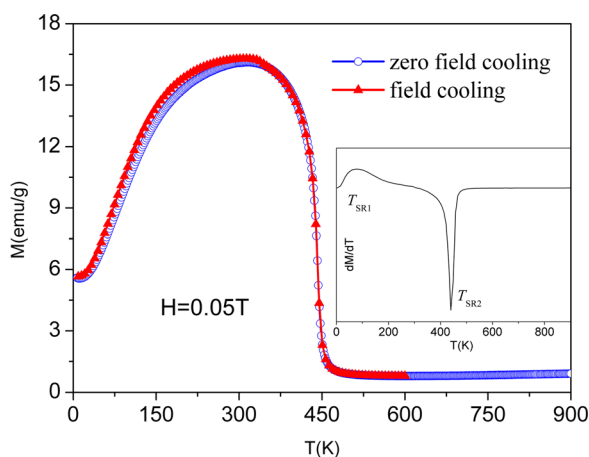


FIG. 2. Temperature dependences of ZFC and FC magnetization for  $\text{GdCo}_9\text{Si}_2$  compound under a magnetic field of 0.05 T. The inset is the differential of zero field cooling  $M$ - $T$  curve.

suggesting the negligible magnetic contribution of the  $\text{Co}_9\text{Si}$  impurity even though its Curie temperature is higher than 900 K. In compounds involving later rare-earth metals (REM) and transition metals (TM), the interaction between TM 3d electrons and REM 5d electrons dominates the magnetic behavior. Such interaction is generally negative and makes the overall 3d-4f spin coupling antiferromagnetic. It has been reported that in the Co-rich Co-REM compounds the onset of long-range magnetic ordering is induced by the 3d-3d interaction in transition metals.<sup>10</sup> Therefore, the abrupt increase of susceptibility when temperature is decreased below 420 K should result from the ordering of Co moments. Further decrease of temperature enhances the interaction of Gd lattice, but the antiferromagnetic interaction between Gd lattice and Co sublattice reduces the net moment. At low temperatures, both sublattices are saturated and the net moment is lowered to a minimum and invariable.

The saturation magnetization of  $\text{GdCo}_9\text{Si}_2$  at 5 K is 9.4 emu/g, which equals  $0.09 \mu_B$  per formula unit, smaller than the value of a free  $\text{Gd}^{3+}$  ion ( $7\mu_B$ ), indicating antiferromagnetic coupling of the Gd and Co moments. With increasing temperature, the saturation magnetization gradually increases up to 29.5 emu/g at 300 K, then decreases at higher temperatures. The insets of Figure 3 show the isothermal magnetization curves  $M(H)$  for  $\text{GdCo}_9\text{Si}_2$  with temperature from 34 K to 316 K and from 329 K to 585 K. Based on the isothermal  $M(H)$  curves and the Maxwell relation, the values of  $-\Delta S_M$  as a function of temperature for a maximum field of 5 T are calculated and shown in Figure 3. It is obvious that the positive and negative  $-\Delta S_M$  peaks for  $\text{GdCo}_9\text{Si}_2$  compounds correspond to the first ( $T_{\text{SR}1}$ ) and second transitions ( $T_{\text{SR}2}$ ), respectively. The value of  $-\Delta S_{\text{Max}}$  at  $T_{\text{SR}2}$  reaches  $1.1 \text{ J}\cdot\text{kg}^{-1}\cdot\text{K}^{-1}$  under 5 T. It is comparable with those of some ferromagnetic materials, such as  $\text{Nd}_{0.9}\text{Dy}_{0.1}\text{Co}_4\text{Al}^{12}$  and  $\text{Fe}_{75}\text{Nb}_{10}\text{B}_{15}$  alloys.<sup>13</sup> The other peak value of  $-\Delta S_{\text{Max}}$  at  $T_{\text{SR}1}$  is  $-0.6 \text{ J}\cdot\text{kg}^{-1}\cdot\text{K}^{-1}$  under 5 T. The refrigerant capacity (RC) is obtained by integrating the area under the  $-\Delta S_M(T)$  curves, using the full temperature width at half maximum

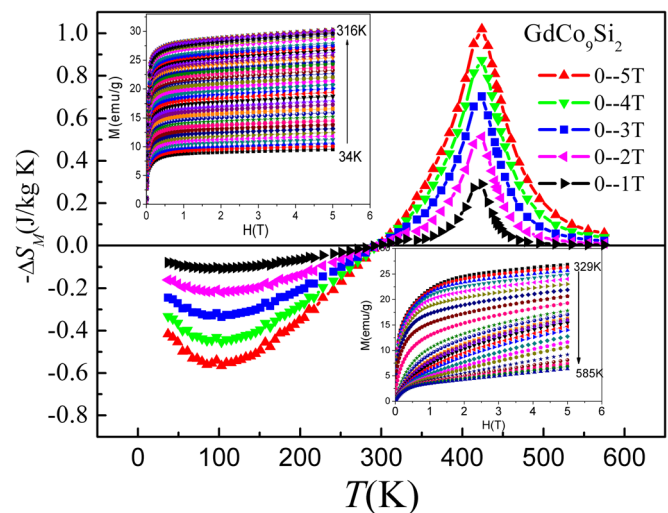


FIG. 3. Magnetic entropy change  $-\Delta S_M$  as a function of temperature in various applied magnetic fields change for  $\text{GdCo}_9\text{Si}_2$  compound. The insets are isothermal magnetization curves.



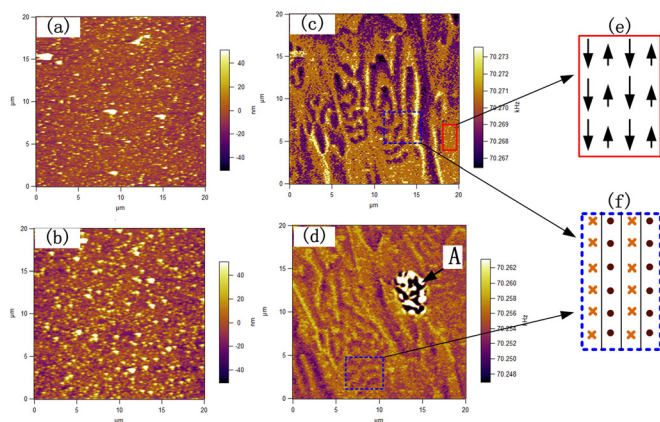


FIG. 4. The AFM (a), (b) and corresponding MFM (c), (d) morphology at room temperature, respectively. (e) and (f) The domain structure is sketched schematically as a top view and a cross-section corresponding to red solid and blue dashed box, respectively.

of the  $-\Delta S_M$  peak as the integration limits. The values of RC at  $T_{SR2}$  are 22 and 62  $\text{J}\cdot\text{kg}^{-1}$  in a field of 2 T and 5 T, respectively.

It is worth mentioning that temperature dependent electrical resistance ( $R$ ) measurements show a metal-semiconductor transition around 260 K, as evidenced by a transition from an increasing  $R$  with increasing temperature ( $T$ ), to a decreasing  $R(T)$  curve, showing a peak at 260 K. This peak is shifted to higher  $T$  when magnetic field is applied, displacing the maximum to higher temperatures outside the experimental temperature range for  $H = 2$  T. A more detailed analysis of the possible influence of this transition on the magnetocaloric response is currently being undertaken and will be reported elsewhere.

From above discussion, one can justify that there is a ferrimagnetic phase near room temperature in  $\text{GdCo}_9\text{Si}_2$  compound. In order to understand the magnetic domain structure, AFM and MFM experiments were performed at room temperature in the tapping or lift mode, as shown in Figure 4. Figure 4(a) presents the AFM image of the sample. The corresponding MFM image, shown in Figure 4(b), is characterized by the stripe and grid structures of  $1\ \mu\text{m}$  wide, as shown in blue dashed box. With knowledge about the ferrimagnetic characterization and the presented AFM micrographs, the magnetic domains are sketched schematically as a top view and cross-section in Figure 4(f). The magnetic moments might display alternating in- and out-of-plane. Except for these structures, there are other type domain areas, such as red solid box, which could be ascribed to the alternating magnetic moments up- and down-of-plane, as shown in Figure 4(e). Figures 4(b) and 4(d) reveal the AFM and MFM images at other zones in the same sample,

respectively. In addition to the stripe domain, there is a zone labeled “A” in which the magnetic domains become very strong. It could be associated to the ferromagnetic impurity phase  $\text{Co}_9\text{Si}$ .

The polycrystalline compound  $\text{GdCo}_9\text{Si}_2$  with  $\text{BaCd}_{11}$  type structure (space group  $I41/amd$ ) has been prepared by arc-melting. The structure, magnetic, and magnetocaloric properties of the compound have been investigated. Two magnetic transitions are observed: one from antiferromagnetic to ferrimagnetic ( $T_{SR1} = 93$  K) and another to paramagnetic order ( $T_{SR2} = 420$  K). There are two peak values in  $-\Delta S_M(T)$ , corresponding to  $T_{SR1}$  and  $T_{SR2}$ , with magnitudes  $-0.6$  and  $1.1\ \text{J}\cdot\text{kg}^{-1}\cdot\text{K}^{-1}$ , respectively, for  $\Delta H = 5$  T. The magnetic domain structures show stripe and grid structures with about  $1\ \mu\text{m}$  wide. It is interesting that the resistivity shows a metal-semiconductor transition at  $\sim 260$  K and to determine its origin theoretical calculations, X-ray photoelectron spectroscopy, and  $\rho(T)$  studies under different magnetic field are in progress.

This work was financially supported by the Guangzhou Municipal Science and Technology Program (Grant No. 12F582080022), the Scientific Research Foundation for the Returned Overseas Chinese Scholars, State Education Ministry (Grant No. x2clB7120290), the Fundamental Research Funds for the Central Universities (Grant Nos. 2011ZM0014 and 2012ZZ0013), and the Guangdong Provincial Science and Technology Program (Grant Nos. 2010B050300008 and 2009B090300273).

- <sup>1</sup>J. H. Belo, A. M. Pereira, J. Ventura *et al.*, *J. Alloys Compd.* **529**, 89–95 (2012).
- <sup>2</sup>L. W. Li, K. Nishimura, H. Igawa *et al.*, *J. Alloys Compd.* **509**, 4198–4200 (2011).
- <sup>3</sup>Z. G. Zheng, X. C. Zhong, H. Y. Yu *et al.*, *J. Appl. Phys.* **109**, 07A919 (2011).
- <sup>4</sup>J. L. Zhang, Z. G. Zheng, W. H. Cao *et al.*, *J. Magn. Magn. Mater.* **326**, 157–161 (2013).
- <sup>5</sup>X. C. Zhong, J. X. Min, Z. G. Zheng *et al.*, *J. Appl. Phys.* **112**(3), 33903 (2012).
- <sup>6</sup>C. Mayer, E. Gaudin, S. Gorsse *et al.*, *J. Solid State Chem.* **184**(2), 325–330 (2011).
- <sup>7</sup>J. Shen, J. F. Wu, and J. R. Sun, *J. Appl. Phys.* **106**, 83902–83906 (2009).
- <sup>8</sup>M. El-Hagary, H. Michor, and G. Hilscher, *J. Magn. Magn. Mater.* **322**(19), 2840–2844 (2010).
- <sup>9</sup>Y. L. Yaropolov, A. S. Andreenko, S. A. Nikitin *et al.*, *J. Alloys Compd.* **509**, S830–S834 (2011).
- <sup>10</sup>M. El-Hagary, H. Michor, S. Özcan *et al.*, *J. Phys. Condens. Matter* **18**, 4567–4580 (2006).
- <sup>11</sup>K. Madono, T. Matsui, S. Kosugi *et al.*, *Nucl. Instrum. Methods Phys. Res. B* **267**, 1604–1607 (2009).
- <sup>12</sup>S. C. Ma, D. H. Wang, C. L. Zhang *et al.*, *J. Alloys Compd.* **499**, 7–10 (2010).
- <sup>13</sup>J. J. Ipus, J. S. Blázquez, V. Franco *et al.*, *J. Appl. Phys.* **105**, 123922–123927 (2009).